Initial Observations of Cold Surge Frequency over Southeast Asia in Relation to ENSO-Induced Anomalies

Ahmad Ridzuan Mohammed Shariff [1,4,*], Mandeep Singh Jit Singh [2,1], Kalaivani Chellappan [2,1], Wayan Suparta [1,2], Fredolin T. Tangang [3], Ester Salimun [3,4], Maszidah Muhammad [2], Mardina Abdullah [1,2], Mohammad Tariqul Islam [2,1]

[1] Space Science Centre (ANGKASA), Institute of Climate Change (IPI)
[2] Department of Electrical, Electronics and Systems Engineering, Faculty of Engineering and Built Environment
[3] School of Environmental and Natural Resource Sciences, Faculty of Science and Technology
[4] Centre for Tropical Climate Change System (IKLIM), Institute of Climate Change (IPI)
Universiti Kebangsaan Malaysia,
43600 Bangi, Selangor, Malaysia.
* ridzuan_s@yahoo.com

***Abstract*—Over the Southeast Asian region, strong surges of cold northeasterly winds are common during winter of the southern hemisphere. For these cold surges, the occurrence frequency is known to vary in conjunction with the El Niño–Southern Oscillation (ENSO) phenomenon. This preliminary study looks at the correlation between cold surge frequency (CSF) and two indicators of ENSO-induced anomalies — the Southern Oscillation Index (SOI) and the Oceanic Niño Index (ONI). ENSO events are detected when each of these indices exceed certain anomaly threshold values for a specified prolonged period. These anomaly threshold values (AT_{SOI} and AT_{ONI}) are used as conditions for logical filtering. Four unrelated rounds of logical filtering are applied to 20 seasons of data. Correlation values are then calculated. The results show that the CSF has a more significant one-to-one correlation with the anomaly of atmospheric pressure (which is indicated by the SOI) than the anomaly of sea surface temperature (indicated by the ONI). However, the findings suggest that the approach of logical filtering using both anomaly indices (together) is more effective, when observing CSF in relation to ENSO. Also, it is suggested that CSF per normal seasons is in the range of 16 to 17 events during DJF. (These results apply to an area between 110° and 117.5°E along 15°N.)**

Keywords – Southeast Asian cold surges; El Niño-Southern Oscillation (ENSO); Southern Oscillation Index (SOI); Oceanic Niño Index (ONI); logical filtering

I. INTRODUCTION

Strong bursts of cold polar winds are a feature of many climate systems around the world [1]. Cold surges, as they are commonly known, are a predominant feature over Southeast Asia during boreal winter [2]. The Southeast Asian cold surges originate from a high pressure anticyclone known as the Siberian High [3] (which as the name suggests, is a climatic feature of the Russian far-north). High pressure build-up in the Siberian High system results in strong bursts of cold polar air being pushed great distances east-southward [4] and reaching the South China Sea. Over the South China Sea, these surges move on as northeasterly winds and bring heavy winter monsoon precipitation [5] to parts of the region, including Thailand [6] and Malaysia [7].

As these cold surges have huge impacts on the regional climate, it is important to study their occurrence frequencies. Various studies have observed variability of the cold surges' occurrence in conjunction with intensity of the El Niño-Southern Oscillation (ENSO) phenomenon [8],[9]. The cold surges' frequency (CSF) have been observed to vary during the two phases of ENSO; namely El Niño and La Niña. CSF has been observed to be extremely low during 'strong El Niño' years. On the other hand, CSF has been observed to be extremely high during 'strong La Niña' years.

Intensities of ENSO phases ('strong'/ 'moderate'/ 'weak') are determined from observations of deviations in certain climatic parameters over a specified prolonged period of time. These deviations from normal conditions are known as anomalies [10],[11]. For ENSO, among the most commonly observed anomalies are for the climatic parameters of atmospheric pressure at sea level (measured by the Southern Oscillation Index - SOI) and sea surface temperature (measured by the Oceanic Niño Index - ONI).

In this respect, the monitoring of ENSO is done through various means. The older indices typically employ in situ observations (station-based data). While the newer methods take advantage of satellite technologies, including satellite-based indices, and GPS meteorology [12],[13]. As the SOI and ONI indices are based on in situ (station) observations, they possess the advantage of having distinctively longer records compared to satellite-based indices [14].

This preliminary study looks at the correlation between CSF and the two abovementioned indicators of ENSO-induced anomalies – the Southern Oscillation Index (SOI) and the

Oceanic Niño Index (ONI). The first objective of this preliminary study is to determine which of the two anomaly indices are most significantly correlated to the CSF in Southeast Asia. The second objective is to determine whether observation of both anomaly indices (together) is more significantly correlated with the Southeast Asian CSF - when compared to observation of only a single anomaly index versus CSF. Finally, the third objective is to determine the CSF range for normal seasons (which are not affected by ENSO).

II. METHODOLOGY AND DATA

A. Determination of the Temporal Scope

This study focuses on winter of the southern hemisphere (boreal winter), similar to the study by Chang et al. [2]. As such, the months under scrutiny are December to February (DJF). A total number of 20 seasons are covered, from 1995/1996 until 2014/2015.

B. Calculation of the Cold Surge Frequency (CSF)

For the purpose of determining the CSF, the essential first step is to define a cold surge index. This study refers to the index defined by Chang et al. [2]. A cold surge index is chosen as the averaged 925-hPa meridional wind between 110° and 117.5°E along 15°N. (Please refer to Figure 1.) According to this definition, a cold surge event happens when the value of this index exceeds 8 ms^{-1}.

The dataset used for the 925-hPa meridional wind parameter is the NCEP/NCAR Reanalysis 1, described in [15]. (NCEP stands for the 'National Centers for Environmental Prediction', while NCAR is the 'National Center for Atmospheric Research'.) This dataset is provided by the NOAA/OAR/ESRL PSD, Boulder, Colorado, USA. Data resolution is at 2.5° X 2.5° sized grids.

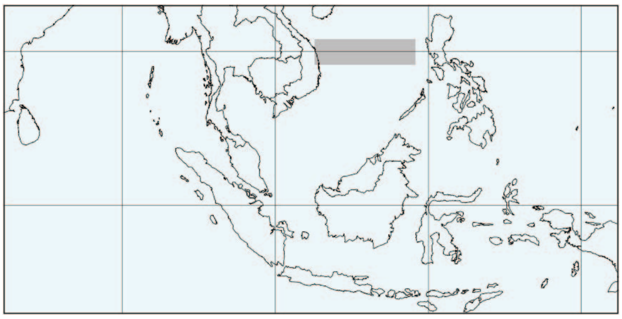

Figure 1. Area for the cold surge index (the rectangular part shaded grey), covering the area from 110° to 117.5°E along 15°N.

C. Sourcing Values for the Southern Oscillation Index (SOI)

Values for the SOI are sourced from the Australian Bureau of Meteorology's 'SOI Archives', which is available at [http://www.bom.gov.au/climate/current/soihtm1.shtml].

The values of -8 and +8 are identified as the anomaly threshold values for SOI (AT_{SOI}). Further explanation regarding AT_{SOI} is presented in Section III of this paper.

D. Sourcing Values for the Oceanic Niño Index (ONI)

Values for the ONI are sourced from NOAA's Climate Prediction Center, available at their website. [http://www.cpc.noaa.gov/products/analysis_monitoring/ensostuff/ensoyears.shtml].

The values of +0.5 and -0.5 are identified as the anomaly threshold values for ONI (AT_{ONI}). Further explanation regarding AT_{ONI} is presented in Section III of this paper.

E. Logical Filtering and Calculation of Correlation

The identified anomaly threshold values (AT_{SOI} and AT_{ONI}) are used as conditions for logical filtering [16]. Logical filtering is a technique adopted from the computing domain of artificial intelligence [17]. For the purposes of this preliminary study, a very basic form of logical filtering is applied.

Four unrelated rounds of logical filtering are applied to 20 seasons of data:

- The first round - $Filter_{SOI}$ - filters and selects seasons which exceed AT_{SOI} only. Then the correlation of CSF in conjunction with SOI is calculated based on results from $Filter_{SOI}$. Figure 2 presents the simplified algorithm.

$Filter_{SOI}$
Condition: AT_{SOI} is less than -8* OR more than +8*.

*Negative (-8): El Niño-related AT_{SOI}.
*Positive (+8): La Niña-related AT_{SOI}.

1. Select Unfiltered Data (20 Seasons).
2. Apply $Filter_{SOI}$.
3. Return Filtered Data.
4. Select Filtered Data.
5. Calculate Correlation: CSF versus SOI.

Figure 2. A natural language representation of the algorithm for $Filter_{SOI}$.

- The second round - $Filter_{ONI}$ - filters and selects seasons which exceed AT_{ONI} only. Then the correlation of CSF in conjunction with ONI is calculated based on results from $Filter_{ONI}$. Figure 3 presents the simplified algorithm.

$Filter_{ONI}$
Condition: AT_{ONI} is more than +0.5* OR less than -0.5*.

*Positive (+0.5): El Niño-related AT_{ONI}.
*Negative (-0.5): La Niña-related AT_{ONI}.

1. Select Unfiltered Data (20 Seasons).
2. Apply $Filter_{ONI}$.
3. Return Filtered Data.
4. Select Filtered Data.
5. Calculate Correlation: CSF versus ONI.

Figure 3. A natural language representation of the algorithm for $Filter_{ONI}$.

- The third round - $Filter_{SOI\ AND\ ONI}$ - filters and selects seasons which exceed both AT_{SOI} and AT_{ONI}. Then the correlation of CSF in conjunction with SOI, and CSF in conjunction with ONI is calculated based on results from Filter$_{SOI\ AND\ ONI}$. Figure 4 presents the simplified algorithm.

Filter$_{SOI\ AND\ ONI}$ [Condition 1: AT_{SOI} is less than -8 OR more than +8] AND [Condition 2: AT_{ONI} is more than +0.5 OR less than -0.5]
1. Select Unfiltered Data (20 Seasons). 2. Apply Filter$_{SOI\ AND\ ONI}$. 3. Return Filtered Data. 4. Select Filtered Data. 5. Calculate Correlation: CSF versus SOI. 6. Calculate Correlation: CSF versus ONI.

Figure 4. A natural language representation: Algorithm for Filter$_{SOI\ AND\ ONI}$.

- Finally, the fourth round - Filter$_{NORMAL}$ - filters and selects seasons which do not exceed both AT_{SOI} and AT_{ONI}. This filtering is done to identify the CSF during 'normal' seasons; seasons which are not affected by ENSO. Figure 5 presents the simplified algorithm.

Filter$_{NORMAL}$ [Condition 1: AT_{SOI} is more than or equal to -8 AND less than or equal to +8] AND [Condition 2: AT_{ONI} is more than or equal to -0.5 AND less than or equal to +0.5]
1. Select Unfiltered Data (20 Seasons). 2. Apply Filter$_{NORMAL}$. 3. Return Filtered Data.

Figure 5. A natural language representation: Algorithm for Filter$_{NORMAL}$.

Results of the data analyses are presented and discussed in Section III.

III. Results and Discussion

A. *Results of Cold Surge Frequency (CSF) Calculations*

Table I presents results of the CSF calculations for the 20 Seasons (DJF). Also presented are their corresponding values of 3-month mean SOI, and 3-month mean ONI. While Figure 6 shows the plot for CSF in comparison with SOI. The shape of the plot shows that CSF is in close general agreement with SOI. Figure 7 on the other hand, shows the plot for CSF in comparison with ONI. In general, the shape of the plot shows that CSF has an opposite phase to ONI.

B. *The Southern Oscillation Index (SOI) and AT_{SOI}*

The SOI is the oldest index used in this study; values are available beginning 1876 to the present. The SOI is the difference between atmospheric pressure at sea level at Tahiti (in French Polynesia) and Darwin (in Australia) [18]. During El Niño, the pressure becomes below average in Tahiti and above average in Darwin, and the Southern Oscillation Index is negative. During La Niña, the pressure behaves oppositely, and the index becomes positive.

When the SOI values are continuously below -8 for prolonged number of months, it often indicates the presence of El Niño. Conversely, when the SOI values are continuously above +8 for prolonged number of months, it indicates the presence of La Niña. As such, the values of -8 and +8 are identified as the anomaly threshold values for SOI (AT_{SOI}).

TABLE I. Results of Cold Surge Frequency (CSF) Calculations

Seasons (DJF)	*CSF (DJF)*	*Mean SOI (DJF)*	*Mean ONI (DJF)*
1995/1996	26	1.33	-0.9
1996/1997	11	8.20	-0.5
1997/1998	5	-17.27	2.2
1998/1999	27	12.50	-1.5
1999/2000	26	10.27	-1.7
2000/2001	19	9.50	-0.7
2001/2002	17	0.43	-0.2
2002/2003	10	-6.67	1.1
2003/2004	16	2.27	0.3
2004/2005	10	-11.77	0.6
2005/2006	15	4.47	-0.9
2006/2007	24	-4.33	0.7
2007/2008	23	16.60	-1.5
2008/2009	23	12.50	-0.8
2009/2010	9	-10.53	1.6
2010/2011	32	23.10	-1.4
2011/2012	25	11.63	-0.9
2012/2013	18	-3.57	-0.6
2013/2014	30	3.83	-0.6
2014/2015	21	-4.23	0.6

Total number of Seasons: 20

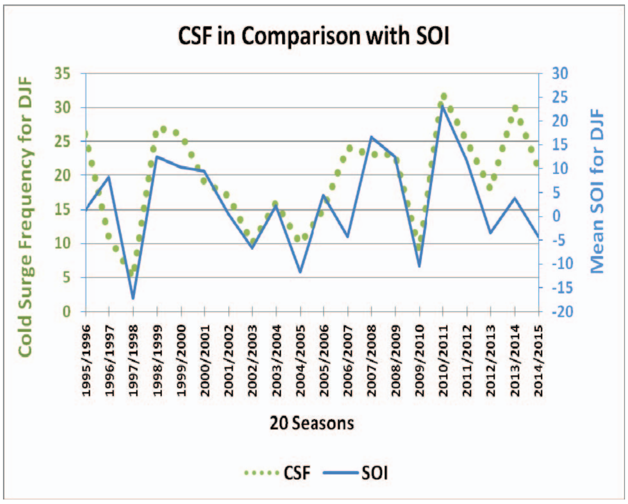

Figure 6. Plot for CSF in comparison with SOI.

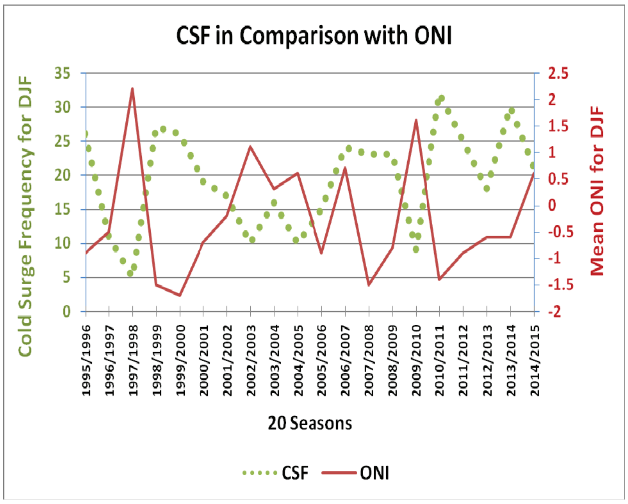

Figure 7. Plot for CSF in comparison with ONI.

C. *The Oceanic Niño Index (ONI) and AT_{ONI}*

The ONI tracks sea surface temperature (SST) anomalies at an area of the Pacific Ocean called 'Niño 3.4' [19]. This index is a running three-month mean anomaly of SST, and is used by NOAA to classify intensity of ENSO episodes ('strong'/ 'moderate'/ 'weak').

When the ONI values are continuously above +0.5 for five consecutive overlapping three-month periods, it indicates the presence of El Niño. On the other hand, when the ONI values are continuously below -0.5 for five consecutive overlapping three-month periods, it indicates the presence of La Niña. As such, the values of +0.5 and -0.5 are identified as the anomaly threshold values for ONI (AT_{ONI}).

D. *Results of Logical Filtering and Correlation Calculations*

Table II presents the correlation values obtained before and after the logical filtering process. The CSF has a direct correlation relationship with SOI and an inverse correlation relationship with ONI.

Before logical filtering is applied, the correlation for CSF and SOI is +0.73, while for CSF and ONI is -0.75. Results after logical filtering show stronger correlation values. For CSF and SOI after $Filter_{SOI}$, the value increases to +0.90. For CSF and ONI after $Filter_{ONI}$, the value increases to -0.79.

However, the most significant results are from the third round of filtering, which is $Filter_{SOI\ AND\ ONI}$. CSF and SOI show a positive correlation of +0.96, while CSF and ONI show a negative correlation of -0.94.

TABLE II. THE CALCULATED CORRELATION VALUES

Filters	*Correlation: CSF and SOI*	*Correlation: CSF and ONI*
Before Filtering	+0.73	-0.75
$Filter_{SOI}$	+0.90	Not Applicable
$Filter_{ONI}$	Not Applicable	-0.79
$Filter_{SOI\ AND\ ONI}$	+0.96	-0.94

Next, Figure 8 is a compilation of scatter plots for each of the cases encountered in this study (before and after filtering is done). The plots on the left are for the three cases of CSF versus SOI. While the plots on the right are for the three cases of CSF versus ONI. Also shown are the respective linear equations, values for the coefficient of determination (R^2), and also the values of the correlation coefficient (R).

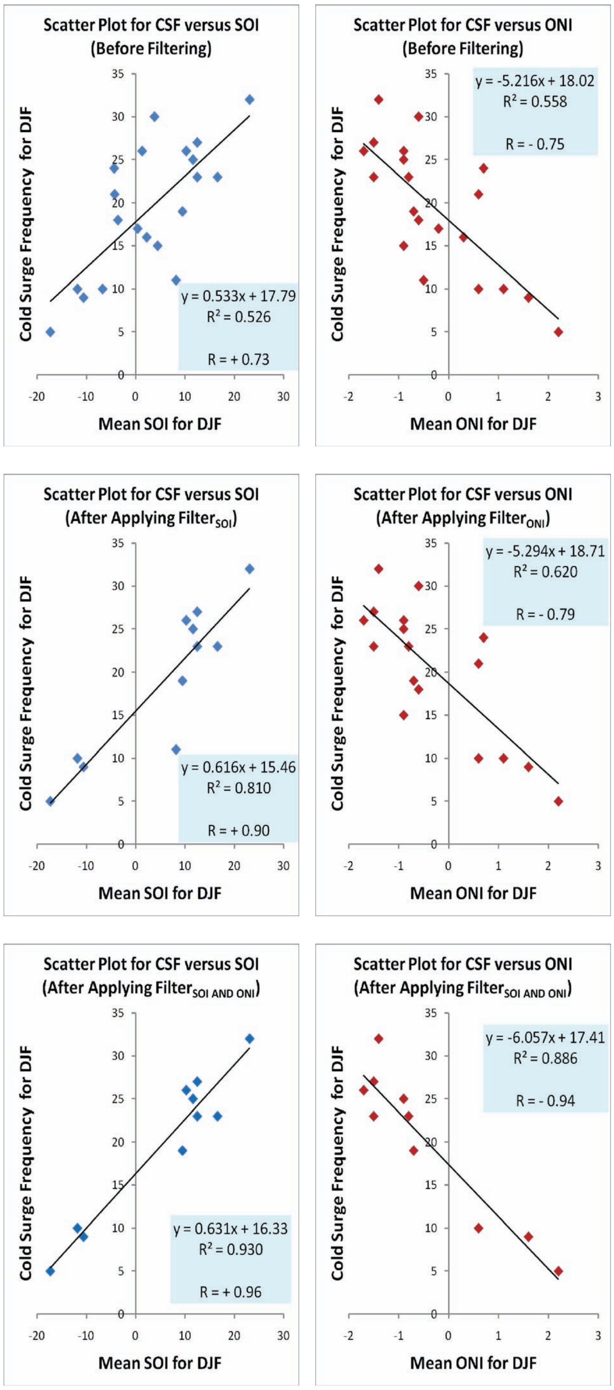

Figure 8. Compilation of scatter plots for each cases.

Finally, Table III lists the results from the fourth round of logical filtering, $Filter_{NORMAL}$. The purpose of this filter is to identify the CSF range during seasons which are not affected by ENSO. Two seasons have been identified which fit this category. For DJF 2001/2002, the CSF value is 17. While for DJF 2003/2004, the CSF value is 16. As such, the results suggest that the CSF range during normal seasons is 16 to 17, for the period being studied.

TABLE III. RESULTS FROM $\text{FILTER}_{\text{NORMAL}}$

Seasons (DJF)	*CSF (DJF)*	*Mean SOI (DJF)*	*Mean ONI (DJF)*
2001/2002	17	0.43	-0.2
2003/2004	16	2.27	0.3

IV. CONCLUSIONS

The first objective of this preliminary study is to determine which of the two anomaly indices are most significantly correlated to the CSF in Southeast Asia.

The results show that the CSF has a more significant one-to-one correlation with the anomaly of atmospheric pressure (which is indicated by the SOI) than the anomaly of sea surface temperature (indicated by the ONI). The correlation values for CSF versus SOI are higher in magnitude (compared to CSF versus ONI) in each of the cases, after logical filtering.

In fact, when the results are filtered for SOI only ($\text{Filter}_{\text{SOI}}$), the correlation value is +0.90. (When filtered for ONI only, the correlation value is -0.79.) This implies that the SOI is the best anomaly indicator to be used for observations of CSF in relation to ENSO (for the region being studied).

The second objective is to determine whether observation of both anomaly indices (together) is more significantly correlated with the Southeast Asian CSF, when compared to observation of only one single anomaly index versus CSF.

The findings do indicate that utilisation of both anomaly indices in the logical filter, yield the highest correlation values in this study (for both indices). As such, the implication is that the approach of logical filtering using both anomaly indices (together) is indeed more effective, when observing CSF in relation to ENSO.

Additionally, this preliminary study also attempted to identify the CSF range during normal seasons. The findings suggest a CSF range of 16 to 17, for the temporal scope of this study. The identification of this range will be useful to determine episodes of above or below normal for cold surge occurrences.

It is important to note that these results apply to the region between 110° and 117.5°E along 15°N. The selection of this region, based on Chang et al. [2], is due to the conciseness and ease of use of this particular definition of cold surge index.

The next step for this study will be to examine the CSF trends on a longer timescale; to identify whether similar patterns emerge. It is also of interest to apply the logical filtering methods to observe CSF in relation to other relevant phenomena - possibly the Madden-Julian Oscillation (MJO) and the Indian Ocean Dipole (IOD).

ACKNOWLEDGMENT

This work is supported by the Malaysian Ministry of Education, under the Project Code: LRGS/TD/2011/UKM/PG/01. NCEP Reanalysis data is provided by the NOAA/OAR/ESRL PSD, Boulder, Colorado, USA. Values for the SOI are sourced from the Australian Bureau of Meteorology's 'SOI Archives', while ONI values are sourced from NOAA's Climate Prediction Center (CPC). Special thanks to Halimatun Muhamad for her assistance, and also to the reviewer(s) which have helped to improve this manuscript.

REFERENCES

[1] Garreaud, René D. "Subtropical cold surges: Regional aspects and global distribution." International Journal of Climatology 21, no. 10 (2001): 1181-1197.

[2] Chang, C. P., Patrick A. Harr, and Hway-Jen Chen. "Synoptic disturbances over the equatorial South China Sea and western Maritime Continent during boreal winter." Monthly Weather Review 133, no. 3 (2005): 489-503.

[3] Panagiotopoulos, Fotis, Maria Shahgedanova, Abdelwaheb Hannachi, and David B. Stephenson. "Observed trends and teleconnections of the Siberian high: A recently declining center of action." Journal of climate 18, no. 9 (2005): 1411-1422.

[4] Jeong, Jee-Hoon, Tinghai Ou, Hans W. Linderholm, Baek-Min Kim, Seong-Joong Kim, Jong-Seong Kug, and Deliang Chen. "Recent recovery of the Siberian High intensity." Journal of Geophysical Research: Atmospheres (1984–2012) 116, no. D23 (2011).

[5] Chen, Tsing-Chang, Jenq-Dar Tsay, Ming-Cheng Yen, and Jun Matsumoto. "The winter rainfall of Malaysia." Journal of Climate 26, no. 3 (2013): 936-958.

[6] Wongsaming, P., and R. H. B. Exell. "Criteria for Forecasting Cold Surges Associated with Strong High Pressure Areas over Thailand during the Winter Monsoon." Journal of Sustainable Energy & Environment 2 (2011): 145-156.

[7] Tangang, Fredolin T., Liew Juneng, Ester Salimun, P. N. Vinayachandran, Yap Kok Seng, C. J. C. Reason, S. K. Behera, and T. Yasunari. "On the roles of the northeast cold surge, the Borneo vortex, the Madden‐Julian Oscillation, and the Indian Ocean Dipole during the extreme 2006/2007 flood in southern Peninsular Malaysia." Geophysical Research Letters 35, no. 14 (2008).

[8] Zhang, Yi, Kenneth R. Sperber, and James S. Boyle. "Climatology and interannual variation of the East Asian winter monsoon: Results from the 1979-95 NCEP/NCAR reanalysis." Monthly Weather Review 125, no. 10 (1997): 2605-2619.

[9] Chen, Tsing-Chang, Wan-Ru Huang, and Jin-ho Yoon. "Interannual variation of the East Asian cold surge activity." Journal of climate 17, no. 2 (2004): 401-413.

[10] Hastenrath, Stefan. "Dipoles, temperature gradients, and tropical climate anomalies." Bulletin of the American Meteorological Society 83, no. 5 (2002): 735-738.

[11] Tangang, Fredolin T., and Liew Juneng. "Mechanisms of Malaysian rainfall anomalies." Journal of climate 17, no. 18 (2004): 3616-3622.

[12] Suparta, Wayan, Ahmad Iskandar, Mandeep Singh Jit Singh, Mohd Alauddin Mohd Ali, Baharudin Yatim, and Fredolin Tangang. "A study of El Niño-Southern oscillation impacts to the South China Sea region using ground-based GPS receiver." In Journal of Physics: Conference Series, vol. 423, no. 1, p. 012043. IOP Publishing, 2013.

[13] Suparta, Wayan, Ahmad Iskandar, Mandeep Singh Jit Singh, Mohd Alauddin Mohd Ali, Baharudin Yatim, and Ahmad Norazhar Mohd Yatim. "Analysis of GPS water vapor variability during the 2011 La

Niña event over the western Pacific Ocean." Annals of Geophysics 56, no. 3 (2013): R0330.

[14] Curtis, Scott, and Robert Adler. "ENSO indices based on patterns of satellite-derived precipitation." Journal of climate 13, no. 15 (2000): 2786-2793.

[15] Kalnay, Eugenia, Masao Kanamitsu, Robert Kistler, William Collins, Dennis Deaven, Lev Gandin, Mark Iredell et al. "The NCEP/NCAR 40-year reanalysis project." Bulletin of the American meteorological Society 77, no. 3 (1996): 437-471.

[16] Amir, Eyal, and Stuart Russell. "Logical filtering." In IJCAI, vol. 3, pp. 75-82. 2003.

[17] Baral, Chitta, and Michael Gelfond. "Logic programming and knowledge representation." The Journal of Logic Programming 19 (1994): 73-148.

[18] Ropelewski, C. F., and P. D. Jones. "An extension of the Tahiti-Darwin southern oscillation index." Monthly Weather Review 115, no. 9 (1987): 2161-2165.

[19] Barnston, Anthony G., Muthuvel Chelliah, and Stanley B. Goldenberg. "Documentation of a highly ENSO-related SST region in the equatorial Pacific." Atmosphere-ocean 35, no. 3 (1997): 367-383.